Interactive comment on "Using GNSS-based vegetation optical depth, tree sway motion, and eddy-covariance to examine evaporation of canopy-intercepted rainfall in a subalpine forest" *by* S. P. Burns et al.

Reply to Referee #4

S. P. Burns et al.

sean@ucar.edu

Date: June 27, 2025

The comments by Referee 4 are greatly appreciated. We have listed the comments by Referee 4 below in italics, followed by our responses. For completeness, we reply to all of Referee 4's comments and have refined/improved the previous replies; therefore, these comments supersede anything that differs from our initial reply to Referee 4 on 6 June 2025.

This research investigates promising and novel techniques to predict rainfall interception and, thus indirectly, canopy evaporation. The authors use L-band microwave active microwave attenuation data (vegetation optical depth) from a GNSS doublet and tree sway data measured by a an accelerometer placed on the trunk of a tree canopy. The study is set in an subalpine, high elevation needleleaf forest in in Colorado/USA. The authors demonstrate the ability of both proxies to correlate with onset and drydown of precipitation events, evapotranspiration and modeled interception storage from different land surface model (CLM4.5) parameterizations. The data sets and analysis presented by the authors allow for the conclusion that these techniques are promising tools to measure interception storage and that they hold potential to supplement/validate land surface models that are known to have high uncertainties in interception fluxes the their parameterization of the canopy, and uncertainties in EC water flux measurements during rain events. This study is of great quality. However, the authors should address the comments below before publication.

This is an accurate summary of our study and we appreciate the positive comments that our study is of "great quality". The specific comments by Referee 4 are replied to below.

Under the category "Major comment":

Please elaborate on the robustness of tree sway motion being able to represent interception storage without the need to account for wind speed as a possible confounding factor. In this context, it would be valuable to find sway motion data as a function of wind speed—e.g. in fig. 10 and at least in one of the plot over time—to clarify on this relationship and include this missing piece of information.

Based on mechanical theory, the natural sway frequency f_{sway} of a conifer tree acts like a damped harmonic oscillator; therefore, it does not depend on wind speed. This is highlighted in Sect.3 of Raleigh et al. (2022) as well as many other studies (e.g., Moore and Maguire, 2004; Van Emmerik et al., 2017; Jackson et al., 2021), who show that f_{sway} is described by the cantilever model:

$$f_{sway} \propto \frac{1}{2\pi} \left(\frac{K}{m} \right)^{0.5}, \tag{1}$$

where K is the flexural rigidity of the tree and m is the mass of the tree, including the branches and

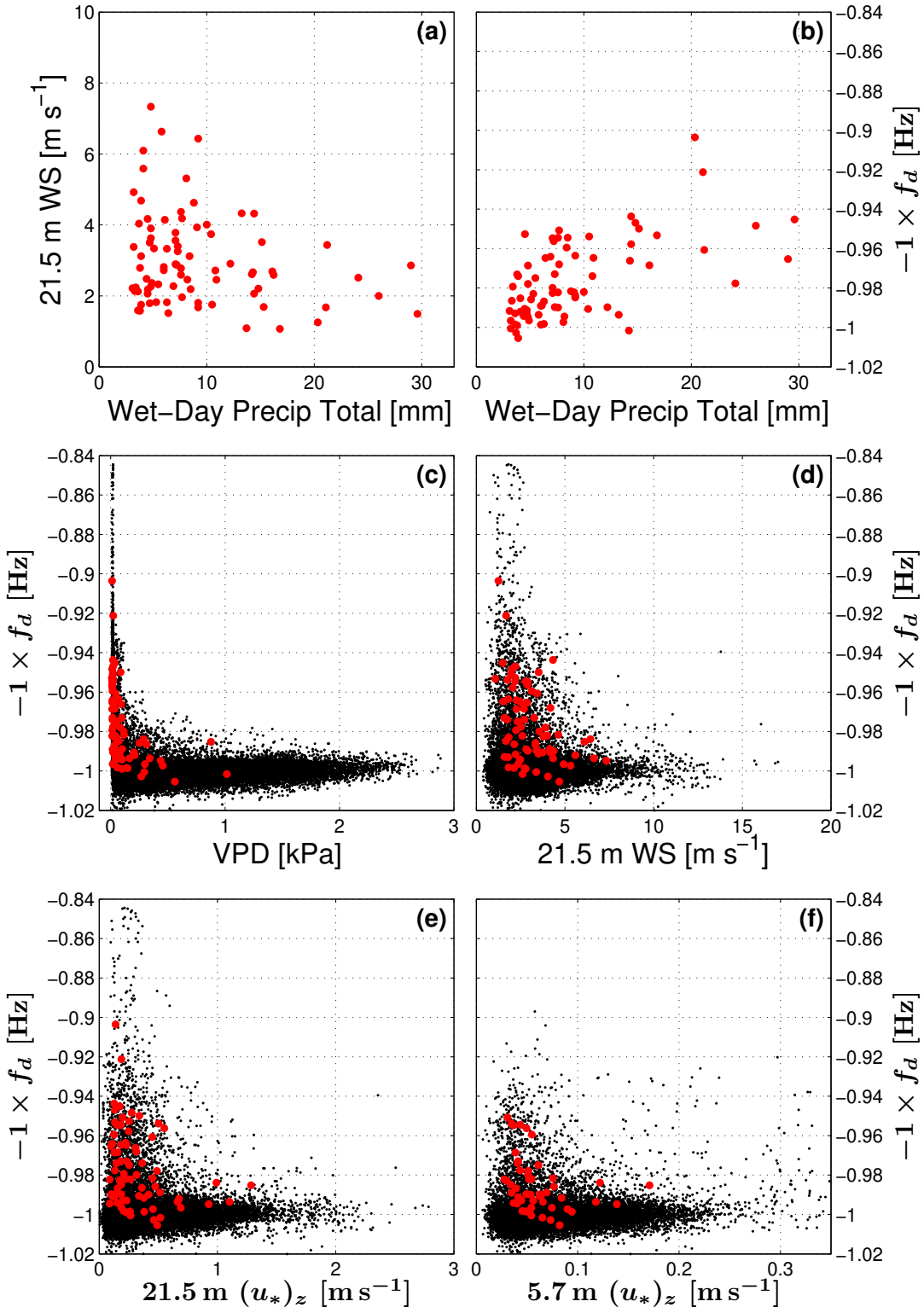

Figure R1: Similar to Fig. 10 in the discussion manuscript, but using detrended tree sway frequency f_d rather than VOD. In **(a)**, the relationship between above-canopy mean horizontal wind speed WS and total precipitation amount from the wet day preceding the wDry day is shown. We have multiplied f_d by -1 to create patterns consistent with VOD (as in Fig. 10). The solid black points are the 30-min mean values from the warm season periods for years 2016 to 2023, the red points are the mean values calculated between 4 and 8 hours after precipitation ended. See Fig. 10 for additional details.

leaves/needles. As precipitation accumulates on the tree leaves and branches, m changes which alters f_{sway}. Therefore, f_{sway} is primarily a structural property of the tree that depends on mass (tree biomass + water in/on the tree), elasticity (which varies with tree temperature, thermal state, and water content), and tree geometry (tree height and DBH). There are other models which are appropriate for other tree types (e.g., simple pendulum for broadleaf trees), but across model types (cantilever and pendulum) tree frequency is not predicted by wind speed.

As alluded to by Referee 4, this technique requires some minimal level of wind speed to generate tree sway. This was mentioned on lines 400-401, as one of the limitations of the method. The lack of a dependence of tree sway on wind speed is discussed in detail in the supplemental material of Raleigh et al. (2022) (see their Fig.S5) as well as the other papers listed above. The mean wind speed impacts the amplitude of oscillations, rather than the frequency (which is what is used in our study). As explained in Raleigh et al. (2022), periods with absolute calm-wind conditions were gap-filled by interpolation. With this said, we agree with Referee 4 that it is worth creating something like Fig. 10, but using tree sway frequency rather than VOD (especially since we have 6 years of tree sway freq data). This new figure is shown in Fig. R1, and many of the relationships between tree sway frequency and other variables (VPD, wind speed, turbulence) are similar to those with VOD. In Fig. R1d, the relationship between tree sway frequency and wind speed is shown and it can be seen that the periods with lower tree sway freq for WS less than 5 m/s correspond to wetter periods (ie, the red dots). The other take-away from Fig. R1d, is that higher winds (and turbulence levels) are less conducive to changes in tree sway frequency, this is either because the rainwater is mechanically blown/shaken off the tree or it does not rain as often in windy conditions (as shown in Fig. R1a). We intend to include Fig. R1 in the revised manuscript with additional discussion about it.

Under the category "Minor comments":

1. Fig 1

1.1 Please report the the inner circle radius (r=20m) as the authors have done for the outer circle

1.2 Please point the reader of fig. 1's caption to what the different footprint circles represent to better understand the results, i.e. what is the main take-away from the inner circle radius (apart from GNSS paucity visualization).

Because comments 1.1 and 1.2 are related, we answer them together. The meaning of the inner footprint was not clear in our submitted manuscript. There are several points and clarifications that we need to add to the footprint discussion in Appendix B. First, we need to clarify that no clear-cut boundary on the VOD footprint location exists. The exact contribution of individual trees to the VOD measurement will depend on the height of the tree and the proximity of the tree to the GNSS antenna. The inner footprint was an attempt to show that trees closer to the subcanopy GNSS antenna contribute more to the VOD flux. In Fig. R2, we have attempted to show this schematically from a side-view perspective of the forest. The tree shading in Fig. R2 shows how the trees closer to the subcanopy GNSS antenna contribute more to the VOD measurement. We intend to include Fig. R2 in the supplemental material of the revised manuscript and improve the text in Appendix B.

1.3 Appendix B, line 527: Please clarify the role of r=20 in this study. Did the authors clip the radius so the "several tall trees" are not included in the footprint?

The inner and outer VOD footprints shown in Fig. 1 are purely conceptual and no trees were removed from the data-processing based on these footprints. A better representation of the areas excluded in the data processing are shown in the skyplot (Fig. S3) where regions were excluded based on the lightning dissipator locations (not based on the trees location or the footprint radius).

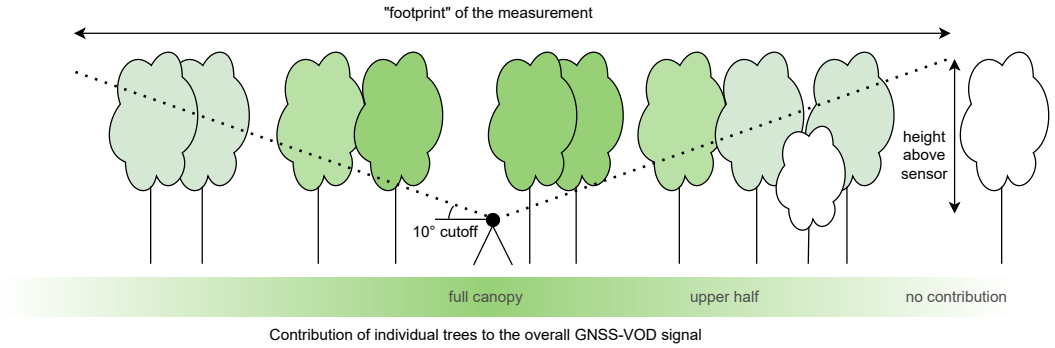

Figure R2: Schematic of how the VOD footprint varies with tree height and distance from the subcanopy GNSS antenna. The trees with darker shading indicate a larger contribution to the VOD footprint.

2. Appendix B & Fig. S3 (GNSS sky view):

2.1 Please show the elevation angle and cutoff to clarify which parts of the canopy will effectively be used for VOD calculation, especially elevation=10°

The schematic in Fig. R2 shows an elevation angle of 10 degrees and which parts of the forest will be used. As discussed above, we plan to include this schematic and additional discussion about it in the revised manuscript.

2.2 Please clarify the rationale behind clipping out another area in NE, close to the northern GNSS gap

There are two lightning dissipators at the top of the tower, so two locations in the skyview are excluded (the lightning dissipators are described in Sect. 2.2.1, lines 130–131 of the discussion manuscript). To clarify what the lightning dissipators look like, photos of them are in Fig. R3.

2.3. You use a very low cutoff elevation angle of 10°. Looking on fig. S3 – assuming the outer two circles being roughly within θ in (10, 30] – only very low VOD can be found that do not display any pattern expected from forest attenuation and possibly fail to represent true forest VOD. Under this light, please explain why the authors used a cutoff=10°.

In principle, the lower the elevation angle, the more homogeneous the VOD should be because it is sampling across a larger number of trees in all directions. Thus, with a high enough canopy, the values at lower elevation angles should converge towards the average VOD at the site, which seems to be the case here (it goes to around 0.4 it seems). Because values from lower elevation angles mainly sample the upper half of the trees, it is true that including them could bias the VOD estimate somewhat, especially if the canopy density is very heterogeneous in the vertical direction. On the other hand, including these low elevations (10–30 deg.) increases the representativity (larger footprint) and the sample size (number of raw measurements), which reduces noise in the VOD time series. It is of course a trade-off, which this study does not aim to explore at this stage.

2.4. Since the Lambert-Beer angle correction assumes a homogeneous canopy and ignores multipath scattering, any losses observed may be due to scattering caused by multiple layers of vegetation, causing Lambert-Beer to break at low angles. Hence, the referee suggests using a higher cutoff elevation angle (∼30 deg.) or would value a discussion why low VOD at lower angles will not affect the overall results. Consider page 12 in Camps et al. (2020) about this question: "Note, however, that only at high elevation angles (elevation angle > 67.5°) is the single scattering albedo correlated with the NDVI, and at lower elevation angles, the presence of multiple scattering makes the tau-omega model [all zeroth order assumption, incl. lambert-beer, ∼the referee] more likely to be invalid."

Thank you for bringing the work by Camps et al. (2020) to our attention. See answer to comment 2.3 above for related details; For our study, the fact that the low elevation values converge to the mean VOD tends to suggest that these values are not so systematically biased that they would need to be removed. We would have acted differently if low elevation values had a different behavior. Though we don't expect the VOD to change much, we agree with Referee 4 that the effect of using a different elevation angle should be further explored. We will recalculate VOD with an elevation angle of 30 degrees to see how it changes the VOD values. This will take a bit of time to do, so we do not have results to share right now, but we plan to include this information in our revised manuscript.

3. 135: Which GNSS frequency is used, please indicate the frequency(ies) in section 2.2.1 since GNSS VOD offers a range of bands to choose from.

Good point. On line 136, the general L-band frequency range (1000-2000 MHz) is described. The specific GNSS frequency used was 1575 MHz which we added to the text near line 136.

4. The authors detrend sway motion to alleviate effects of temperature and vegetation water content on short-term changes. However, VOD is also affected by long-term changes in biomass, and vegetation water content. Why did the authors not consider detrending VOD, especially since a trend is visible in fig. 2? This is worth noting in 2.2.1.

Any low-frequency trend in VOD appears to be much smaller than that of tree sway frequency (i.e., compare the VOD time series in Fig. 2b to that of tree sway frequency in Fig. 2c). Since removing the low-frequency trend in tree sway frequency did not affect the results, we have assumed that removing any low-frequency trend in VOD will also have a minimal effect on the results. We have added text about not removing any low-frequency trend in VOD to Sect. 3.1, where the time series are discussed.

5. 433/4: The size of the EC footprint has not been explicitly mentioned in the text. Also, which footprint size of VOD as your referring to in this statement? To make a statement about the footprint size (a very relevant discussion) the referee suggests to state that although the footprint sizes between all technique partly or greatly differed, the good correlations could be found etc.

We thank Referee 4 for noticing this shortcoming. Shortly after making the submission, the lead author realized that though we make reference the ET flux footprint, we did not include any specific details about it. We appreciate that this oversight was noticed by Referee 4, and will include the following information in the revised manuscript. First, we will cite Chu et al. (2021) who show a footprint climatology and suggest that the US-NR1 footprint has a size of around 500 m^2, but depends on wind direction and atmospheric stability. A more explicit view of the US-NR1 flux footprint climatology is shown below for five different atmospheric stability conditions for winds from the west (Fig. R4) and for winds from the east (Fig. R5). The data are separated into east and west wind directions because winds at the site are typically either upslope (from east) or downslope (from west). For comparison purposes, we include the larger VOD footprint from Fig. 1 on the same plot. The tower footprints have been calculated using the simple footprint model of (Kljun et al., 2015). For the revised manuscript, we plan to include Figs. R4 and R5 within the supplemental material

and add a description of the ET flux footprint to Appendix B. One important difference between the VOD and flux footprints that we will emphasize: the flux footprint location varies with wind direction and atmospheric stability whereas the VOD footprint is unaffected by these variables.

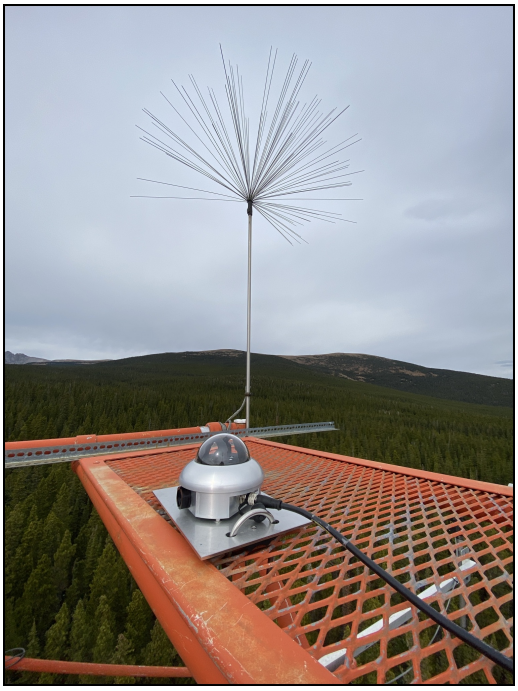

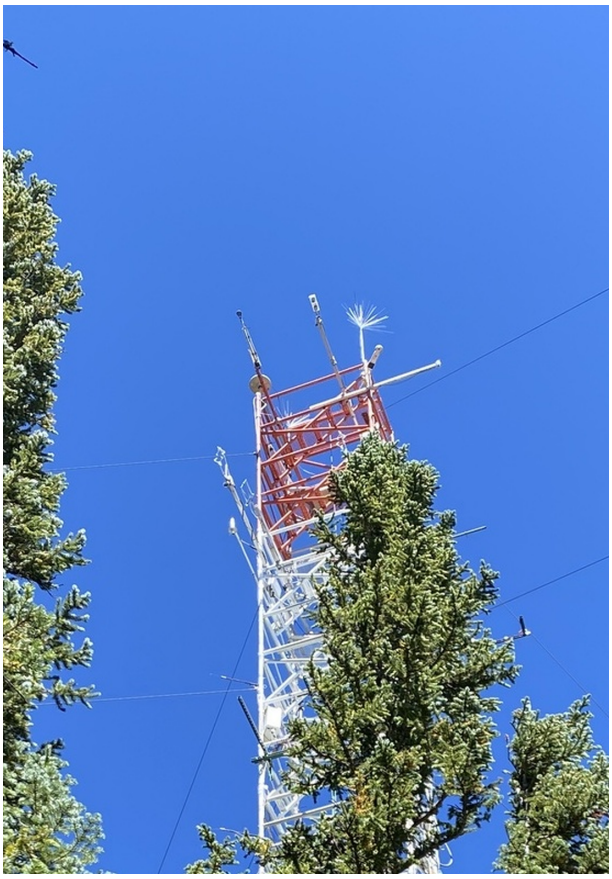

Figure R3: Photos of the lightning dissipators at the top of the US-NR1 flux tower. The right-side photo shows the gnssA antenna on the southwest corner (left/front corner in photo) of the tower and the lightning dissipator on the southeast corner (right corner in photo) of the tower. There is 2nd lightning dissipator on the northwest corner that is barely visible in the right photo, but is the one shown in the left-side photo. The dissipators extend about 2 m above the top of the tower.

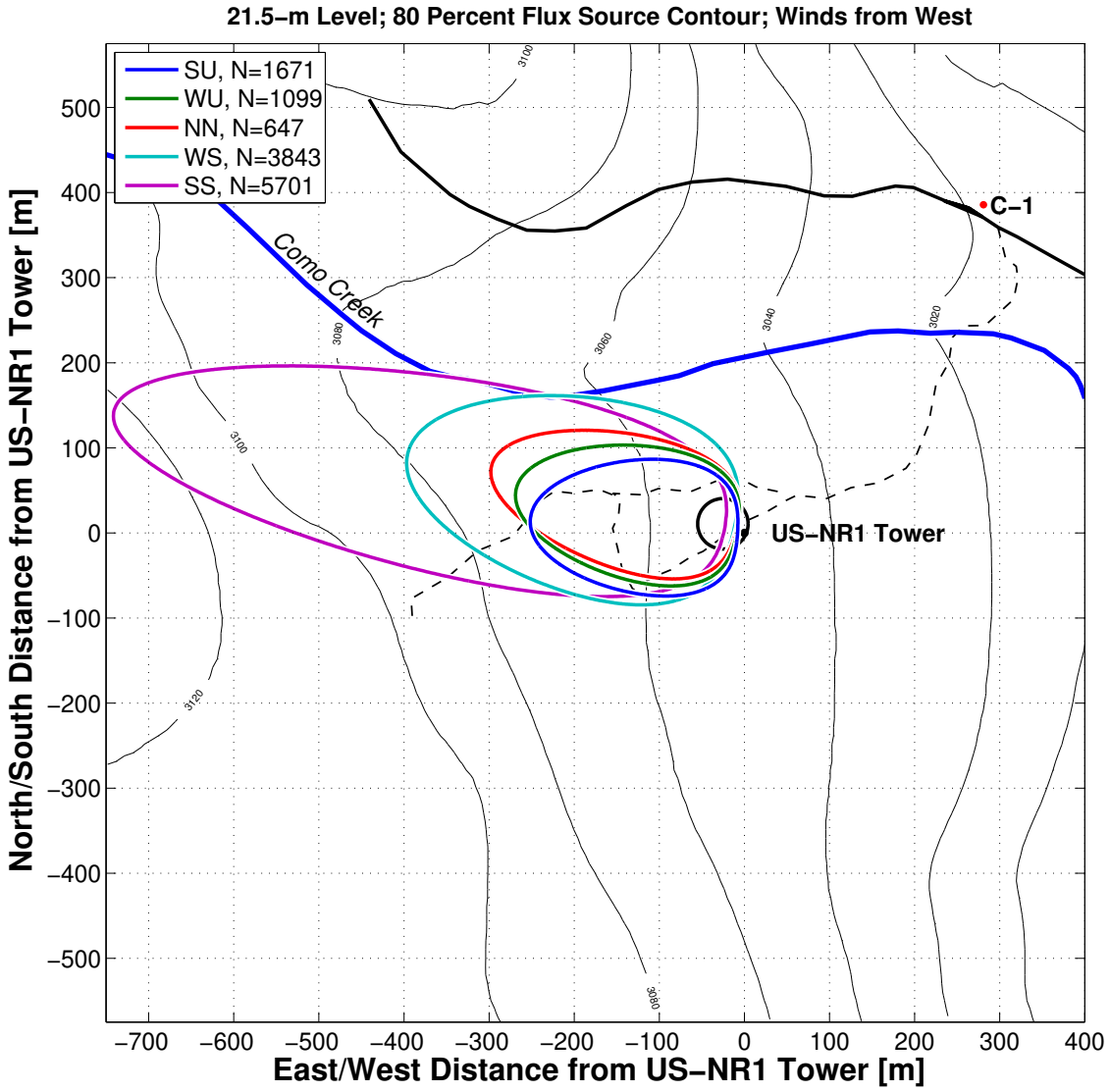

Figure R4: Climatology of the footprint region from which 80% of the 21.5 m turbulent scalar flux originates are shown for winds from the west for different stability classes (SU, strongly unstable; WU, weakly unstable; NN, near-neutral; WS, weakly stable; SS, strongly stable). These are US-NR1 data from July for years 1999–2023 where the number of 30-min samples within each stability category are shown by N in the legend. Footprints are calculated based on Kljun et al. (2015) and shown as distance [meters] from the main US-NR1 flux tower. The larger VOD footprint from Fig. 1 is shown as a black circle.

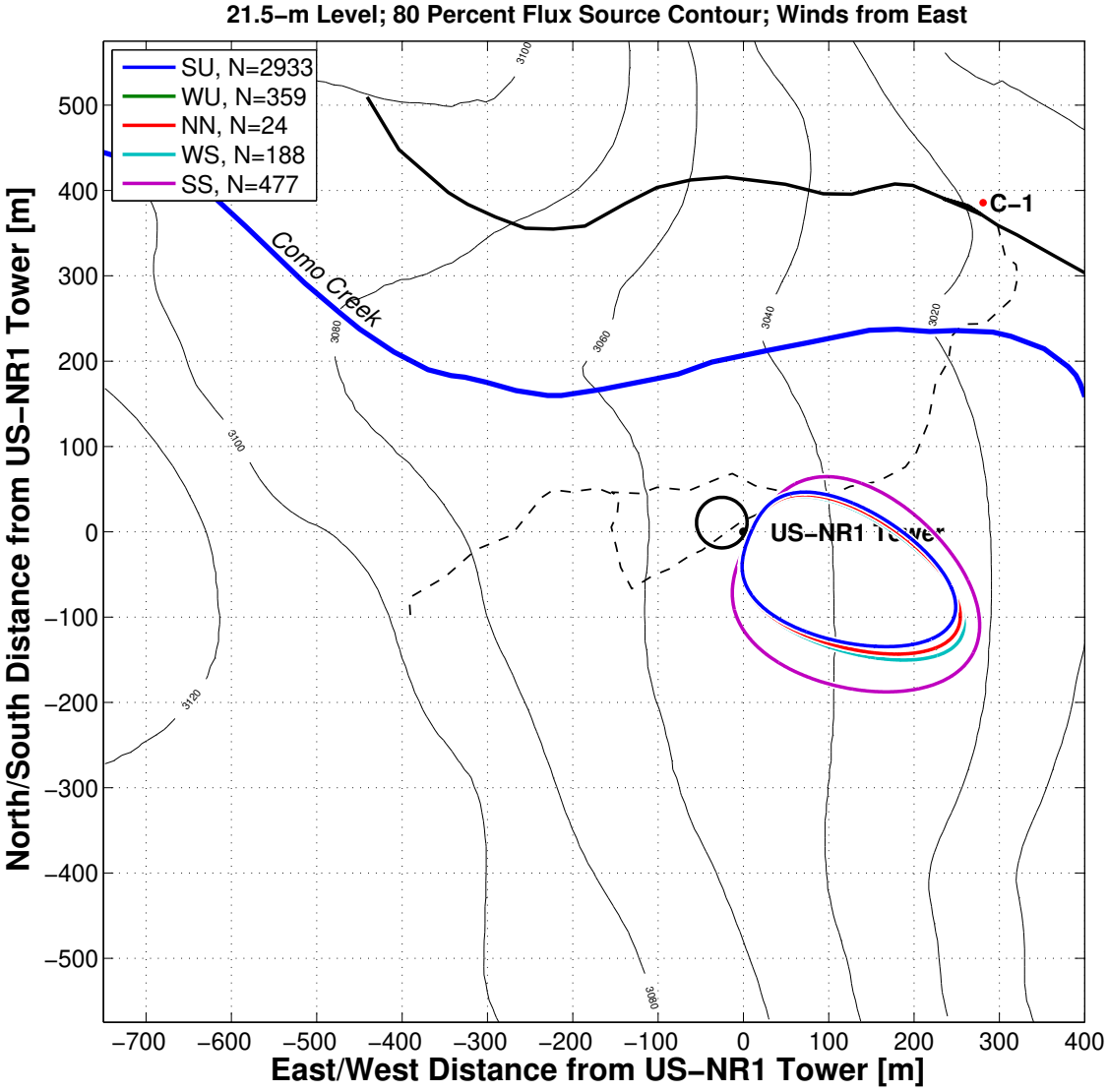

Figure R5: As in Fig. R4, but for winds from the east.

References

Camps, A., Alonso-Arroyo, A., Park, H., Onrubia, R., Pascual, D., and Querol, J.: L-Band vegetation optical depth estimation using transmitted GNSS signals: Application to GNSS-reflectometry and positioning, Remote Sensing, 12, doi:10.3390/rs12152352, 2020.

Chu, H., Luo, X., Ouyang, Z., Chan, W. S., Dengel, S., Biraud, S. C., Torn, M. S., Metzger, S., Kumar, J., Arain, M. A., Arkebauer, T. J., Baldocchi, D., Bernacchi, C., Billesbach, D., Black, T. A., Blanken, P. D., Bohrer, G., Bracho, R., Brown, S., Brunsell, N. A., Chen, J., Chen, X., Clark, K., Desai, A. R., Duman, T., Durden, D., Fares, S., Forbrich, I., Gamon, J. A., Gough, C. M., Griffis, T., Helbig, M., Hollinger, D., Humphreys, E., Ikawa, H., Iwata, H., Ju, Y., Knowles, J. F., Knox, S. H., Kobayashi, H., Kolb, T., Law, B., Lee, X., Litvak, M., Liu, H., Munger, J. W., Noormets, A., Novick, K., Oberbauer, S. F., Oechel, W., Oikawa, P., Papuga, S. A., Pendall, E., Prajapati, P., Prueger, J., Quinton, W. L., Richardson, A. D., Russell, E. S., Scott, R. L., Starr, G., Staebler, R., Stoy, P. C., Stuart-Haëntjens, E., Sonnentag, O., Sullivan, R. C., Suyker, A., Ueyama, M., Vargas, R., Wood, J. D., and Zona, D.: Representativeness of eddy-covariance flux footprints for areas surrounding AmeriFlux sites, Agricultural and Forest Meteorology, 301-302, 108 350, doi:10.1016/j.agrformet.2021.108350, 2021.

Jackson, T. D., Sethi, S., Dellwik, E., Angelou, N., Bunce, A., van Emmerik, T., Duperat, M., Ruel, J.-C., Wellpott, A., Van Bloem, S., Achim, A., Kane, B., Ciruzzi, D. M., Loheide II, S. P., James, K., Burcham, D., Moore, J., Schindler, D., Kolbe, S., Wiegmann, K., Rudnicki, M., Lieffers, V. J., Selker, J., Gougherty, A. V., Newson, T., Koeser, A., Miesbauer, J., Samelson, R., Wagner, J., Ambrose, A. R., Detter, A., Rust, S., Coomes, D., and Gardiner, B.: The motion of trees in the wind: A data synthesis, Biogeosciences, 18, 4059–4072, doi:10.5194/bg-18-4059-2021, 2021.

Kljun, N., Calanca, P., Rotach, M. W., and Schmid, H. P.: A simple two-dimensional parameterisation for Flux Footprint Prediction (FFP), Geosci. Model Dev., 8, 3695–3713, doi:10.5194/gmd-8-3695-2015, 2015.

Moore, J. R. and Maguire, D. A.: Natural sway frequencies and damping ratios of trees: Concepts, review and synthesis of previous studies, Trees, 18, 195–203, doi:10.1007/s00468-003-0295-6, 2004.

Raleigh, M. S., Gutmann, E. D., Van Stan, J. T., Burns, S. P., Blanken, P. D., and Small, E. E.: Challenges and capabilities in estimating snow mass intercepted in conifer canopies with tree sway monitoring, Water Resources Research, 58, doi:10.1029/2021WR030972, 2022.

Van Emmerik, T., Steele-Dunne, S., Hut, R., Gentine, P., Guerin, M., Oliveira, R. S., Wagner, J., Selker, J., and Van de Giesen, N.: Measuring Tree Properties and Responses Using Low-Cost Accelerometers, Sensors, 17, doi:10.3390/s17051098, 2017.